ELSEVIER

Polymer 40 (1999) 4431–4436

polymer

Polymer Communication

Flow-induced birefringence of linear and long chain-branched metallocene polyethylene melts subject to steady start-up flow

C.K. Chai*, J. Creissel, H. Randrianantoandro

BP Chemicals S.N.C., Research and Technology Centre, Boîte Postale no. 6, 13117 Lavéra, France

Received 6 March 1998; received in revised form 17 November 1998; accepted 17 November 1998

Abstract

Optical birefringence induced during steady start-up shear flow of linear and long chain-branched metallocene linear low density polyethylene (LLDPE) melts, and their blends, were investigated at 200°C. Experiments were performed on a high temperature shearing cell, with a pair of parallel quartz plate windows, mounted on a rheometrics optical analyser which employs a rapid polarisation modulation technique for optical anisotropy measurements. The influence of long chain branching (LCB) on chain orientation and stretch were examined at a constant molecular weight (Mw) and molecular weight distribution (MWD), in terms of the amount of non-linear transient response (stress overshoots) and the steady-state value of the flow-induced birefringence of these polymers. Stress overshoots (hence molecular stretch) were found to occur at lower rates in polymers containing LCB than in linear polymers. © 1999 Elsevier Science Ltd. All rights reserved.

Keywords: Birefringence; Orientation; Polyethylene

1. Introduction

Various techniques [1–10] have been developed to characterise chain orientation, segmental stretch, microstructure formation and other morphological changes in various polymeric systems during flow. These include wide angle X-ray scattering (WAXS), Raman spectroscopy, small angle light scattering (SALS), infrared dichroism and birefringence. Birefringence is a measure of anisotropy in the refractive index of a material. In polymer melts, such anisotropy arises to a large extent from anisotropy in the total polarisability which, in turn, is a function of the local orientation of polymer molecules. For flexible polymer chains, the relationship between the anisotropic part of the refractive index tensor (n) and the orientation of molecules is often described by [5]:

$$n = K(\alpha_{//} - \alpha_{\perp})\langle RR\rangle \qquad (1)$$

where K is a constant, $(\alpha_{//} - \alpha_{\perp})$ is the local anisotropy in the polarisability of a polymer segment and $\langle RR\rangle$ is the second-moment of the end-to-end vector orientation distribution. Thus, by measuring the flow-induced anisotropy in the refractive index of macromolecules, one can directly obtain their average angle of segmental orientation and their degree of alignment and stretch. In addition, the stresses in the melts can also be investigated with the birefringence measurements, via the stress-optical rule [6,7]. This rule assumes that the deviatoric components of the refractive index tensor of the flowing sample are proportional to those of its stress tensor. For a simple shear flow $v = \dot{\gamma}(x_2, 0, 0)$ where $\dot{\gamma}$ is the shear rate, the stress-optical rule states that:

$$\tau_{12} = (\Delta n/2C)\sin 2\chi \qquad \text{and} \qquad \tau_{11} - \tau_{22} = (\Delta n/C)\cos 2\chi \qquad (2)$$

where τ_{12} and $(\tau_{11} - \tau_{22})$ are the shear stress and first normal stress differences, respectively, Δn is the birefringence in the flow plane, C is the stress-optical coefficient and χ is the orientation angle. It is well known that the birefringence of polyethylene [6] follows this stress-optical relation and we have independently verified that it holds for the polymers studied in this paper.

We have previously used rheo-X-ray and rheo-Raman techniques [1,2] for the studies of flow-induced orientation and crystallisation on high density polyethylene melts. In this paper, we report on the flow-induced birefringence measurements of LLDPE melts under a steady start-up flow. The overall objective of this work is to investigate the effects of molecular structure on flow-induced

---

* Corresponding author. Tel.: + 33-442-42-94-47; Fax: + 33-442-42-94-45.

E-mail address: chaic@bp.com (C.K. Chai)

PII: S0032-3861(98)00802-7

Table 1
Polymer blend composition and their characteristics relaxation time

Polymer	Type	Relaxation time
PE1	Linear metallocene LLDPE	0.022
80% PE1 + 20% PE2	Blend 1	0.031
60% PE1 + 40% PE2	Blend 2	0.033
40% PE1 + 60% PE2	Blend 3	0.047
20% PE1 + 80% PE2	Blend 4	0.058
PE2	Long chain-branched metallocene LLDPE	0.072

orientability of polymer chains during processing and how the latter influences the crystallisation kinetics during subsequent cooling, leading to its modification of the solid-state morphology and orientation which, in turn, have a strong impact on physical properties (e.g. optical and mechanical). This paper presents the initial results performed on linear and long chain-branched narrow MWD *metallocene* LLDPEs and their blends, concentrating on the influence of LCB, at constant Mw and MWD, on segmental chain orientation and stretch. The complete work that includes Mw and MWD effects, as well as relaxation and crystallisation measurements after cessation of flow, will be reported later.

2. Experimental

Birefringence measurements were performed using a rheometrics optical analyser (ROA). This instrument uses a polarisation modulation technique[5,8] which allows optical anisotropies to be measured rapidly. An He–Ne laser was used to generate light with a wavelength of 632.8 nm. The sample is placed between two circular quartz windows, of a high temperature parallel disk shearing cell, which are in close thermal contact with a silver block heater. The temperature range of this flow cell is between ambient and

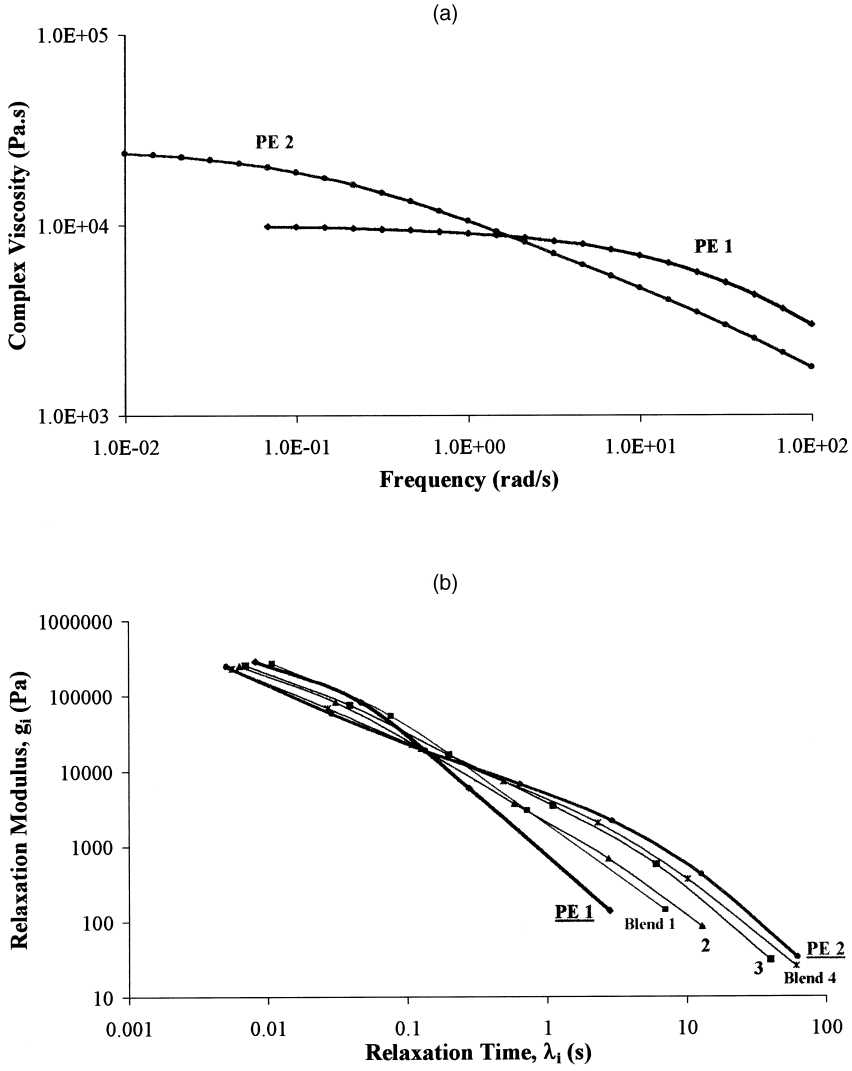

Fig. 1. (a) The magnitude of complex viscosity, $\eta^*(\omega)$ of PE1 and PE2 at 190°C. (b) Relaxation times spectra, calculated using IRIS ™ software package for PE1, PE2 and their blends, at 190°C.

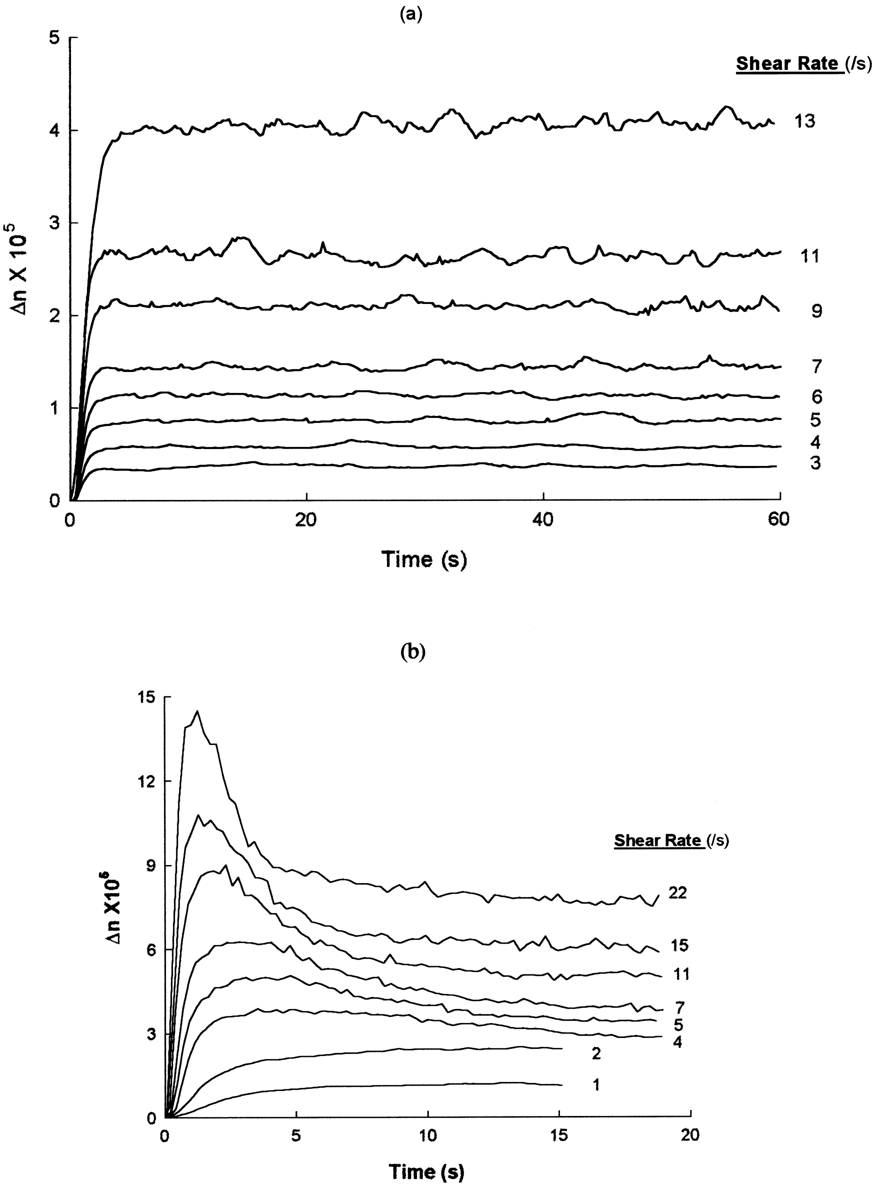

Fig. 2. Time-dependent birefringence on inception of shear for: (a) PE1; and (b) PE2, at different shear rates, at 200°C.

400°C, and a shear rates range of 0.05 to 100 s^{-1}. The gap between the windows can be varied from 10 to 2500 μm and is controlled by a second stepper motor. After the optical components are aligned and calibrated, flow birefringence experiments are conducted under the control of a personal computer (PC). The ROA instrument produces the following signals:

$$R_1 = -\cos 2\theta \sin\delta \quad \text{and} \quad R_2 = \sin 2\theta \sin\delta \qquad (3)$$

where the angle, θ, defines the direction of orientation of the principal axis of refractive index tensor in the plane normal to the axis of light propagation and δ is the retardation which is related to the birefringence in that same plane as:

$$\Delta n = \frac{\lambda}{2\pi d}\delta = \frac{\lambda}{2\pi d}\arcsin\left[\sqrt{R_1^2 + R_2^2}\right] \qquad (4)$$

where d is the optical path length and λ is the wavelength. For the parallel plate mode, as used in this study, the measured birefringence is in the 1–3 plane: i.e. $\Delta n_{13} = C(\tau_{11} - \tau_{33}) = C(N_1 + N_2)$, where N_1 and N_2 are, respectively, the first and second normal stress differences.

Birefringence measurements at several shear rates were performed at 200°C on two *metallocene* LLDPE samples, labelled PE1 and PE2, of different molecular structure, which were analysed by size exclusion or gel permeation chromatography (SEC or GPC) [11]. PE1 is a linear copolymer whose weight average molecular weight (M_w) is 1.0×10^5 with a molecular weight distribution (M_w/M_n) of 2.2, while PE2 is a lightly long chain-branched copolymer, of similar M_w and MWD as PE1, with an LCB parameter $g'_{LCB} = 0.92$ as calculated

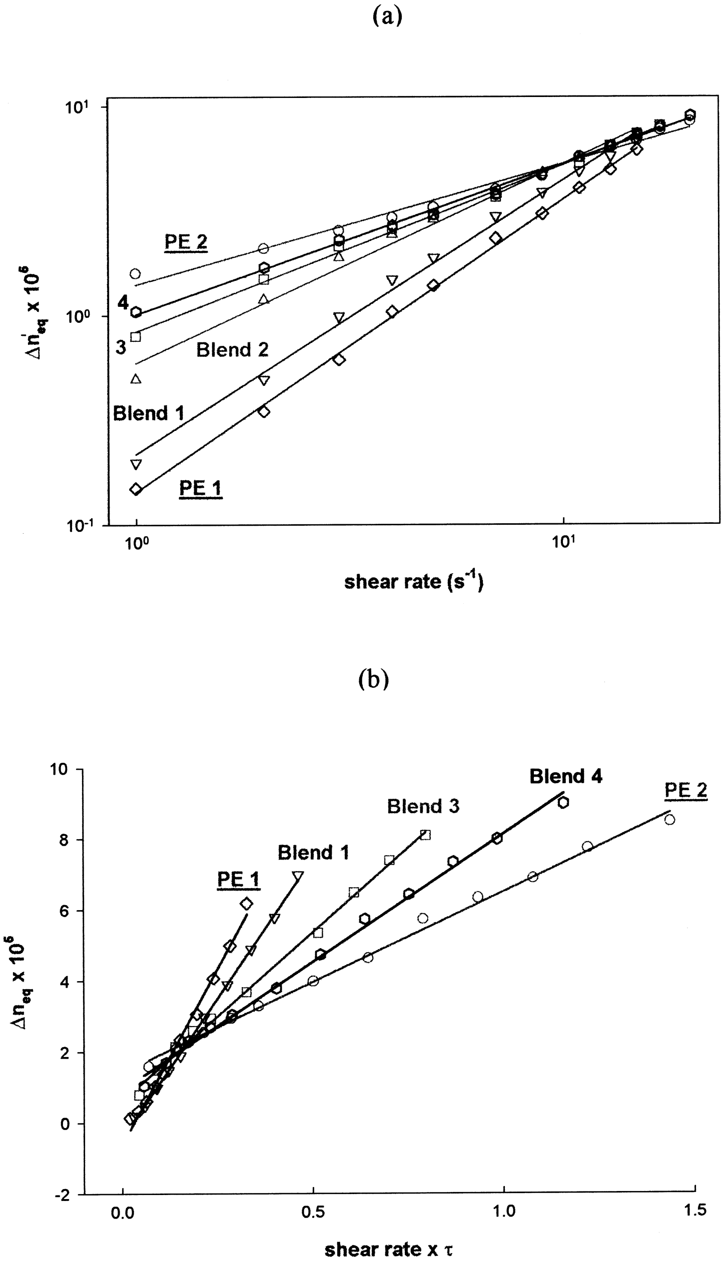

Fig. 3. Steady-state birefringence as a function of: (a) shear rates; and (b) normalised shear rates, for PE1, PE2 and their blends, at 200°C.

from GPC and intrinsic viscosity data [11]. These samples were also characterised by linear dynamic oscillatory shear experiments with a commercial rheometrics RDS rheometer. Frequency sweep experiments at 190°C and 15% strain in parallel plate mode were run under nitrogen from 0.01 to 100 rad s^{-1}.

Blend 1 to Blend 4 (Table 1) were melt blended at different weight ratios of PE1 with PE2 using a single-screw Brabender PL2000 extruder. The specimen was then compression-moulded at 190°C from pellets and slow cooled to room temperature in the press under pressure. A typical specimen size was 25 mm in diameter and 1 mm in thickness.

3. Results and discussion

3.1. Linear dynamic rheology

Fig. 1(a) shows the plot of the magnitude of the complex viscosity $\eta^*(\omega)$ against frequency (ω) for PE1 and PE2 at 190°C. The $\eta^*(\omega)$ curves of the blends which fan between

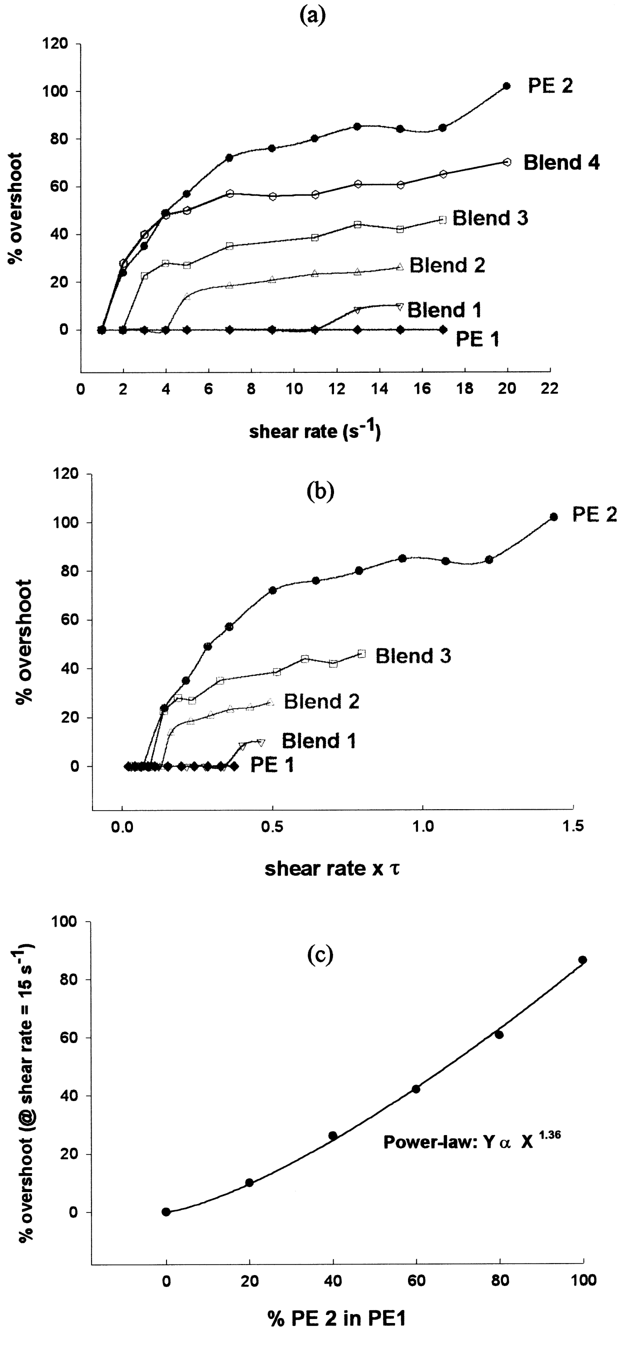

Fig. 4. Percentage overshoot in birefringence as a function of: (a) shear rates; (b) normalised shear rates, for PE1, PE2 and their blends, at 200°C; and (c) as a function of % PE2 in PE1.

those of PE1 and PE2 were omitted in the plot for clarity reason. The differences in the flow curves between PE1 and PE2 signify the influence of LCB in improving the processability of the latter, with a large increase in low shear rates viscosity and stronger shear thinning at high shear rates, while maintaining the same optical and mechanical properties of the former. The stronger shear thinning exhibited by LCB-containing polymers (Blends 1–4 through to PE2) can be interpreted in terms of the ''branch point withdrawal'' mechanism [12,13] which allows long chain-branched molecules to change their relaxation times during flow.

Fig. 1(b) shows the relaxation times spectra, analysed using the commercially available IRIS™ software package, for PE1, PE2 and their blends. The plot shows that the relaxation times spectrum of PE1 span to long relaxation times with an increasing amount of LCB (i.e. the wt.% of PE2 being added to PE1, viz. Blends 1 to 4 through to PE2). This is further shown by the increase in the effective characteristic relaxation times (τ) with LCB, calculated from the ratio of the zero shear rate viscosity to the plateau modulus, as summarised in Table 1.

3.2. Time-dependent birefringence responses

Fig. 2(a) shows the time-dependent birefringence, $\Delta n_{13}(\dot{\gamma}, t)$, of the *linear* narrow MWD metallocene LLDPE (PE1) developed during start-up shear flow, at various shear rates, at 200°C. Typically, the birefringence increases monotonically, without overshoot (up to the maximum shear rates studied), before reaching its steady-state value.

Fig. 2(b) shows the $\Delta n_{13}(\dot{\gamma}, t)$ curves of the lightly *long-chain branched* metallocene LLDPE (PE2) developed during similar shear start-up flow experiments. At low shear rates, $\Delta n_{13}(\dot{\gamma}, t)$ profiles of PE2 are similar to those of PE1. However, at higher shear rates, it passes through a maximum before decreasing to a steady-state value. This non-linear $\Delta n_{13}(\dot{\gamma}, t)$ of PE2 develops at very low shear rates with the overshoot peak narrowing and skewing towards shorter times with increasing shear rates. The $\Delta n_{13}(\dot{\gamma}, t)$ curves of the blends are intermediate to those shown in Fig. 2, e.g. Blend 1 with 20% PE2 starts to exhibit overshoot at $\dot{\gamma} > \backsim 10\ \mathrm{s}^{-1}$.

Such an overshoot in $\Delta n(\dot{\gamma}, t)$ upon inception of flow is a phenomenon that has previously been seen in polymer solutions [4,5,9,10]. There are two cases of overshoots that occur at: (i) constant strain; and (ii) constant time after start-up. The former was thought to reflect the orientation of the chain due to entanglements in a timescale shorter than the disentanglement time. The larger overshoots that occur at constant time after start-up and at higher shear rates than the former are usually associated with the stretch of polymer segments [14,15].

3.3. Steady-state birefringence responses

The steady-state birefringence $\Delta n_{\mathrm{eq}}(\dot{\gamma})$ of the materials studied are double-log plots against shear rate, as shown in Fig. 3(a), while Fig. 3(b) shows the linear plot against dimensionless shear rate $\dot{\gamma} \cdot \tau$, which is defined as the product of the shear rate and the effective relaxation time (τ) in each polymer (Table 1). This dimensionless parameter is also known as the Deborah number ($De = \tau/t$), which can be used to characterise structure–property–processing relationships. The chain orientation in the finished article and, therefore, its contribution to its solid state morphology and physical properties will be dictated by the level of residual shear stress that is able to relax during the melt state process. The higher the Deborah number, the higher the stress that remains unrelaxed, leaving the longest chains aligned in the flow direction during subsequent crystallisation after cessation of flow.

As the stress–optical rule holds for these polymers, the plots show that the developed shear stresses of the branched materials are very different in their dependence on shear rates compared with those of the linear metallocene polymer, e.g. the power index of the plot in Fig. 3(a) decreases with increasing LCB, from 1.4 for PE1 to 0.58 for PE2. At the terminal times zone, $\Delta n_{13}(\dot{\gamma})$ is expected to vary with the square of the shear rate, i.e. $\Delta n_{13}(\dot{\gamma}) \propto \dot{\gamma}^2$; it is clear from Fig. 3(a) that this has not been reached even for the narrow MWD ($M_w/M_n = 2.2$) linear PE1 polymer with a power index of 1.4.

3.4. Non-linear responses

The variation of the overshoot in birefringence, $\Delta n(t)$ with shear rates is summarised in Fig. 4, where the % overshoot is defined as $[\Delta n_{\max}(\dot{\gamma}) - \Delta n_{\text{eq}}(\dot{\gamma})]/\Delta n_{\text{eq}}(\dot{\gamma}) \times 100\%$, which is plotted as a function of shear rate [Fig. 4(a)] and dimensional shear rate [Fig. 4(b)]. The most pronounced feature observed is that no observable overshoot in the birefringence is apparent for the *linear* metallocene polymer (PE1) over the same shear rate range studied. The percentage overshoot for the LCB-containing materials increase monotonically and appear to reach their steady-state values at high shear rates or Deborah numbers. At high shear rates, the stress overshoot appears to follow a power-law relationship with the percentage PE2 blended in PE1 (e.g. the power index is 1.36 at a shear rate of 15 s^{-1}) [Fig. 4(c)], suggesting the segmental stretch increases strongly with the presence of LCB. In particular, the critical shear rate for the onset of stress overshoots shifts to lower shear rates from Blends 1–4 through to PE2 (i.e. as the amount of LCB increases), showing the influence of certain aspects of LCB architecture (in terms of length, placement and topology) in the process of molecular orientation and stretch of polymer segments that occur at constant time after shear start-up flows.

4. Conclusions

The *linear* and *narrow* MWD *metallocene* polymer does not appear to show stress overshoot in birefringence upon inception of flow, over the shear rate range studied. This is an interesting observation, showing the importance of long and branched molecular chains in the process of orientation and stretch during flow. Stress overshoots (hence, molecular stretch) were found to occur at lower rates in polymers containing LCB than in linear polymers.

Acknowledgements

The authors thank BP Chemicals for permission to publish this work and Professor Wagner of IKT and Professor McLeish of Leeds University for helpful discussions. The reviewers comments are also greatly appreciated.

References

[1] Pople JA, Mitchell GR, Chai CK. Polymer 1996;37:4187.
[2] Chai CK, Dixon NM, Gerrard DL, Reed W. Polymer 1995;36:661.
[3] Kornfield JA, Fuller GG, Pearson DS. Macromolecules 1989;22:1334.
[4] Zebrowski BE, Fuller GG. J Polym Sci Polym Phys Ed 1985;23:575.
[5] Fuller GG. Optical rheometry of complex fluids. Oxford: Oxford University Press, 1995.
[6] Janeschitz-Kriegl H. Polymer melt rheology and flow birefringence. New York: Springer, 1983.
[7] Wales JLS. The application of flow birefringence to rheological studies of polymer melts. Rotterdam: Delft University, 1976.
[8] Fuller GG, Mikkelsen JK. J Rheol 1989;33:761.
[9] Pearson DS, Kiss AD, Fetters LJ. J Rheol 1989;33:517.
[10] Menezes EV, Graessley WW. J Polym Sci Polym Phys Ed 1982;20:1817.
[11] Lesec J. J Liquid Chromatogr 1994;17:1029.
[12] Bick DK, McLeish TCB. Phys Rev Lett 1996;76(14):2587.
[13] McLeish TCB, Larson RC. J Rheol 1998;42(1):82.
[14] Mead DW, Leal LG. Rheol Acta 1995;34(4):339.
[15] Pearson DS, Herbolzheimer EA, Marrucci G, Grizzuti N. J Polym Sci Phys Ed 1991;29:1589.